

well as polymer and surface. See, for example, the definition of $\bar{\epsilon}$ preceding Eq. (40) of FH-2.

In the plateau region, on the other hand, adsorption was predicted to be molecular weight independent. Considering the approximations involved, it would probably be more realistic to simply assert that molecular weight dependence is small. The predicted increase in the adsorption plateau with increasing temperature can be easily explained. At higher temperatures the adsorbed polymer coils are more extended normal to the adsorbing surface accommodating more polymer

molecules in the interface at complete surface coverage. Or, putting it another way, at higher temperatures each adsorbed polymer molecule contacts fewer adsorption sites, thus requiring more polymer to completely occupy all sites.

Additional numerical examples and discussion will be presented in a forthcoming publication.⁸

⁸ Comparisons will also be made with other polymer adsorption theories: H. L. Frisch and R. Simha, *J. Chem. Phys.* **27**, 702 (1957); E. R. Gilliland and E. B. Gutoff, *J. Phys. Chem.* **64**, 407 (1960).

Iterative Method for Solution of the One-Dimensional Wave Equation: Eigenvalues and Eigenfunctions for L-J (12, 6) and Exponential (α , 6) Interatomic Potentials*

HALSTEAD HARRISON AND RICHARD B. BERNSTEIN

Chemistry Department, University of Michigan, Ann Arbor, Michigan

(Received 18 December 1962)

A method of direct numerical integration of the one-dimensional wave equation is described and illustrated by calculations of the radial wavefunctions, vibrational energy levels, and numbers of bound states for diatomic molecules. Within the validity of the Born-Oppenheimer approximation, the procedure yields arbitrarily accurate eigenvalues. Several potentials involving long-range, inverse-sixth-power attractions are examined. Results are compared with those from the first-order WKB integral and with the Dunham form of the second-order WKB approximation.

INTRODUCTION

DESPITE recent progress, the problem of deriving interatomic potentials from first principles remains formidable.¹ Nevertheless, spectroscopic data, the numerous transport properties for atomic systems, and scattering experiments can be correlated in terms of empirical potentials. Many such potentials have been proposed, and found useful in special cases.² Guided by evidence from atomic beam scattering³⁻⁵ as well as spectroscopic data,⁶ however, we wish to restrict consideration to potentials for which the long-range part varies as r^{-6} . This dependence is of crucial importance in controlling the energy levels of the higher vibrational states and the total number of bound states. Unfortunately, the special potentials for which exact, or nearly exact, analytical solutions are available do not have the required long-range form. Consequently, numerical methods are necessary to compute precise

eigenvalues and eigenfunctions for "realistic" potentials.

The present paper describes an iterative procedure for direct integration of the radial Schrödinger equation, which yields eigenvalues of arbitrarily high accuracy. The method is illustrated by application to several potentials. Parallel computations by the first-order WKB approximation and by the Dunham version of the second-order WKB method have also been carried out in order to assay the precision and applicability of these simpler methods.

Some Preliminary Considerations

Within the framework of the Born-Oppenheimer approximation, the nuclear and electronic wavefunctions may be separated. The equation for radial wavefunctions describing the nuclear motion may be written in the reduced form:

$$(d^2 Y/dz^2) + B_z [K - V_{\text{eff}}^*(z)] Y = 0, \quad (1)$$

where $z = r/r_m$, $Y(z) = zR(z)$, $B_z = 2\mu\epsilon r_m^2/\hbar^2$, $K = E/\epsilon$, $V^*(z) = V(z)/\epsilon$, and

$$V_{\text{eff}}^*(z) = V^*(z) + [B_z^{-1}l(l+1)]/z^2.$$

In the above, $R(r)$ is the radial wavefunction; r_m is the position of the minimum in the interatomic po-

* Support of this work by the U. S. Atomic Energy Commission, Division of Research is gratefully acknowledged.

¹ A. D. McLean, A. Weiss, and M. Yoshimine, *Rev. Mod. Phys.* **32**, 211 (1960).

² D. Steele, E. R. Lippincott, and J. T. Vanderslice, *Rev. Mod. Phys.* **34**, 239 (1962).

³ F. A. Morse and R. B. Bernstein, *J. Chem. Phys.* **37**, 2019 (1962).

⁴ R. Helbing and H. Pauly, *Z. Physik* (to be published).

⁵ H. Pauly, *Z. Naturforsch.* **15A**, 277 (1960).

⁶ H. W. Woolley, *J. Chem. Phys.* **37**, 1307 (1962).

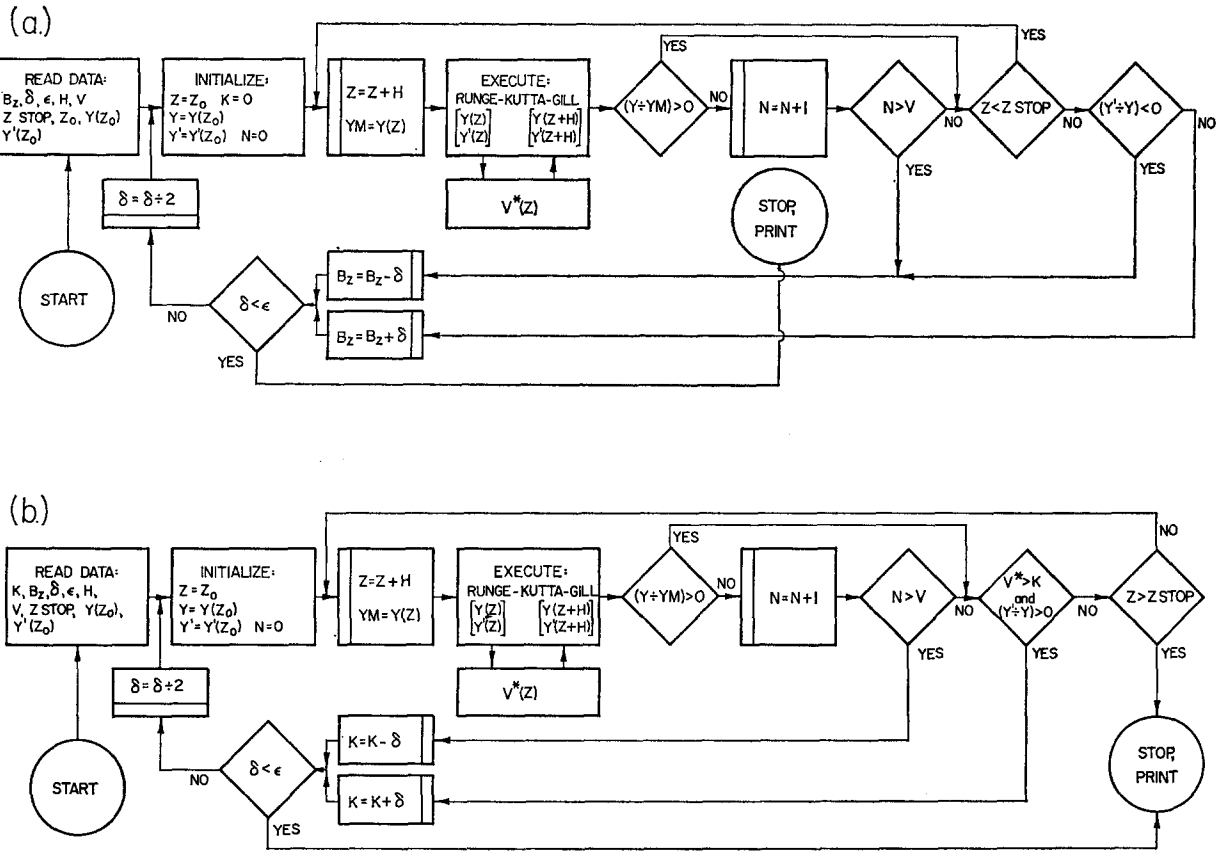


FIG. 1. Computer flow diagrams: (a) B_r -crit(v). (b) $-K(v)$.

tential; μ is the reduced mass; and ϵ is the depth of the well. E is an eigenenergy satisfying the boundary conditions for bound states: $0 = Y(0) = Y'(0) = Y(\infty) = Y'(\infty)$, and K is the "reduced" eigenenergy. B_z is a dimensionless quantity related to the spectroscopic constant B_e , by $B_z = (B_e hc / \epsilon)^{-1}$, and l is the orbital

quantum number (conventionally written J for bound systems).

We will consider the following reduced potentials: the radial harmonic oscillator,

$$V^*(z) = -1 + \frac{1}{2}k(z-1)^2, \quad \text{H.O.}(k)$$

the Morse,

$$V^*(z) = -1 + \{1 - \exp[-\eta(z-1)]\}^2, \quad \text{Morse}(\eta)$$

the family of Lennard-Jones ($n, 6$) potentials,

$$V^*(z) = [6/n-6]z^{-n} - [n/(n-6)]z^{-6}, \quad \text{L-J}(n, 6)$$

and the family of exponential ($\alpha, 6$) potentials,

$$V^*(z) = [6/(\alpha-6)] \exp[-\alpha(z-1)] - [\alpha/(\alpha-6)]z^{-6}. \quad \text{exptl}(\alpha, 6)$$

TABLE I. B_r -critical.

v	L-J (12.000,6)	Exptl. (12.000,6)	Exptl. (13.772,6)	Exptl. (15.000,6)	Morse (6)
0	7.07	6.34	7.18	7.73	9.00
1	46.6	44.1	48.9	51.8	81.0
2	121.3	115.2	127.6	134.9	225.0
3	231.1	219.9	243.4	257.1	441.0
4	376.0	358.0	396.2	418.4	729.0
5	556.1	529.6	586.2	618.8	1089.0
6	771.3	734.8	813.0	858.4	1521.0
7	1021.7	973.5	1077.0	1137.0	2025.0
8	1307.1	1245.6	1378.1	1454.7	2601.0
9	1627.7	1551.2	1716.1	1811.6	3249.0
10	1983.5	1890.3	2091.3	2207.5	3969.0
11	2374.4	2262.9	2503.4	2642.6	4761.0

TABLE II. Empirical expansion coefficients for B_r -crit(v).

	$B_r\text{-crit} \cong A(v + \frac{1}{2})^2 + B(v + \frac{1}{2}) + C \pm 0.1.$		
	A	B	C
L-J (12.000,6)	17.567	4.409	0.47
Exptl (12.000,6)	16.748	4.163	0.07
Exptl (13.772,6)	18.522	4.673	0.22
Exptl (15.000,6)	19.554	4.869	0.50

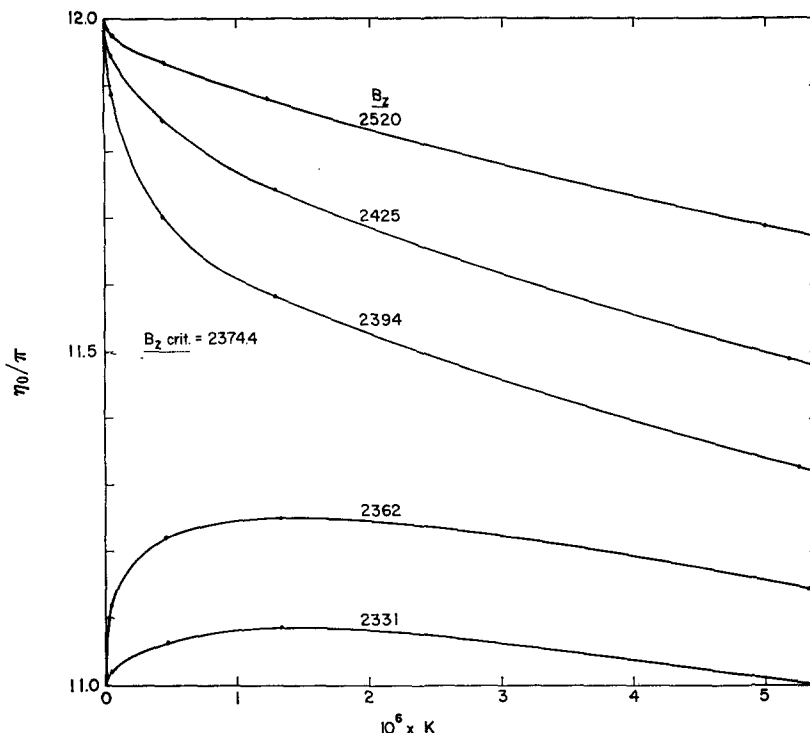


FIG. 2. Phase-shift extrapolations for L-J (12, 6); $v=11 \rightarrow 12$.

For intercomparison, the potentials may be matched to have common curvature at $z=1$, a condition which tends to superimpose the lower energy levels, or the L-J and exp potentials may be matched to coincide asymptotically at large z , a condition which tends to superimpose the uppermost energy levels and the total number of bound states. The former condition requires: $k=2\eta^2=6n=6\alpha(\alpha-7)/(\alpha-6)$; the latter requires $n=\alpha$. For illustration, we have chosen to match the potentials by the first condition to the curvature of the L-J(12,6), i.e., $d^2V^*(z)/dz^2=72$, so that $k=72$, $\eta=6$, $n=12$, and $\alpha=13.772$. Some results for $\alpha=12$ and 15 are also presented.

Two computations have been performed for each potential: (a) calculation of the critical values of B_z [designated $B_z\text{-crit}(v)$] for which the potential just contains the v th vibrational state; and (b) calculation, for several values of B_z , of sets of reduced eigenenergies, ($-K$). In both computations l has been set equal to zero, though the method is general for all l .

COMPUTATION

The method employed is similar to that of Hartree,⁷ modified to take advantage of machine computation⁸ (IBM 7090). A trial value of B_z or K is assumed, the interior boundary conditions set, and a trial wavefunction generated by a Runge-Kutta-Gill numerical

integration. The asymptotic behavior of the trial wavefunction is then compared with the exterior boundary conditions to guide the choice of the next trial value of B_z or K . Iterating, B_z or K is adjusted by successively smaller amounts until the desired precision is reached. This precision is then confirmed by systematic variation of the starting conditions and integration interval.

TABLE III. Eigenenergies for $B_z=2500$. Entries are $-K$ ($\pm 5 \times 10^{-6}$). Potentials are matched to common curvature at $z=1$.

v	L-J(12,6)	Exptl. (13.772,6)	Morse(6)	H.O. (72)
0	0.884165	0.884095	0.883605	0.880000
1	0.679395	0.677375	0.672395	0.640000
2	0.507665	0.502845	0.489995	0.400000
3	0.366555	0.359075	0.336395	0.160000
4	0.253525	0.244255	0.211595	
5	0.165885	0.156065	0.115595	
6	0.100765	0.091705	0.048400	
7	0.055125	0.047835		
8	0.025725	0.020745		
9	0.009155	0.006475		
10	0.001845	0.000925		
11	0.000035			

⁷ D. R. Hartree, Proc. Cambridge Phil. Soc. **24**, 105 (1928).

⁸ R. A. Buckingham and J. W. Fox, Proc. Roy. Soc. (London) **A267**, 102 (1962); a procedure very similar to ours is applied to nuclear bound states by R. S. Caswell, National Bureau of Standards Tech. Note #159 (1962).

TABLE IV. Reduced eigenenergies for Lennard-Jones (12,6) potential. Entries are $-K$.

v	$B_z=10\,000$			$B_z=2500$			$B_z=900$			$B_z=100$		
	Eigen	WKBJ	Dunham	Eigen	WKBJ	Dunham	Eigen	WKBJ	Dunham	Eigen	WKBJ	Dunham
0	0.941045	0.9412	0.94105	0.884165	0.8843	0.88417	0.811515	0.8121	0.81152	0.500965	0.5053	0.50092
1		0.8302	0.83000	0.679395	0.6796	0.67941	0.507175	0.5076	0.50718	0.052085	0.0525	0.05435
2		0.7279	0.72765	0.507665	0.5078	0.50768	0.287845	0.2880	0.28795			(0.02992)
3	0.633695	0.6339	0.63369	0.366555	0.3365	0.36661	0.141505	0.1415	0.14214			
4		0.5478	0.54786	0.253525	0.2535	0.25370	0.054895	0.0547	0.05719			
5		0.4701	0.46984	0.165885	0.1658	0.16636	0.013335	0.0131	0.01966	Values in parentheses are spurious upper states predicted by the Dunham procedure.		
6	0.399295	0.3992	0.39933	0.100765	0.1006	0.10188	0.000775	0.0005	0.01527			
7		0.3363	0.33602	0.055125	0.0549	0.05742			(0.02885)			
8		0.2800	0.27960	0.025725	0.0256	0.03004						
9	0.229515	0.2302	0.22974	0.009155	0.0090	0.01671						
10		0.1864	0.18610	0.001845	0.0016	0.01425						
11		0.1478	0.14835	0.000035	0.0001	0.01940						
12	0.115225	0.1165	0.11614			(0.02876)						
18	0.012345	0.0125	0.01895									

Critical Values of B_z

Figure 1(a) presents a simplified flow diagram for the computation of the critical values of B_z .⁹ Omitted from the diagram is a procedure which changes the integration step, H , so that an approximately constant number of cuts is taken along each halfwavelength. Within the accuracy of the computation (± 0.1 in B_z) results are invariant when 20 or more cuts are evaluated in each halfwavelength. The schedule of z intervals for $v=2$ was used as well for $v=0$ and 1, since for these v the shortest half-wavelength is infinite.

Initial conditions were usually taken to be $Y(0.65) = 10^{-30}$ and $Y'(0.65) = 6.65 \times 10^{-28}$, values whose ratio can be approximated from the WKBJ waveform for the L-J (12, 6) potential. However, no effect upon computed values of B_z -crit was observed when the initial conditions were either $Y(0.65) = 0$ and $Y'(0.65) = 10^{-30}$, or $Y(0.65) = 10^{-30}$ and $Y'(0.65) = 0$, conditions which should generate results high and low, respectively. The parameter ZSTOP was typically 100. The results were not sensitive to ZSTOP when this number exceeded 50.

Computed values of B_z -crit are collected in Table I. The values for the Morse potential agree with the results from the analytical expression^{10,11}

$$B_z\text{-crit} = \eta^2 \left(v + \frac{1}{2}\right)^2. \quad (2)$$

Computed, but omitted from the table, were values of B_z -crit(v) for the harmonic oscillator potential,

⁹ For conventions see: D. McCracken, *Digital Computer Programming* (John Wiley & Sons, Inc., New York, 1951).

¹⁰ P. M. Morse, *Phys. Rev.* **34**, 57 (1929); see also the remarks of D. Ter Haar, *ibid.* **70**, 222 (1946).

¹¹ N. Bernardes and H. Primakoff, *J. Chem. Phys.* **30**, 691 (1959).

H.O.(72), which also agreed with the appropriate analytical expression:

$$B_z\text{-crit} = 2k \left(v + \frac{1}{2}\right)^2. \quad (3)$$

The calculated values of B_z -crit(v) for the remaining potentials can be fitted empirically to expressions of the form:

$$B_z\text{-crit} = A \left(v + \frac{1}{2}\right)^2 + B \left(v + \frac{1}{2}\right) + C.$$

Table II presents the fitted constants.

Alternate Procedure for Confirmation of Critical B_z

As a check on the computational procedure for B_z -crit(v), the number of bound states for several different B_z values was determined by the application of Levinson's theorem,¹² which makes use of scattering phase shifts for various positive energies. Extrapolation of the s -wave phases $\eta_0(K)$ to zero energy yields a value for the number, n , of bound states of zero angular momentum: $n = \eta_0(0)/\pi$. Figure 2 shows such a plot for the L-J(12, 6) potential, with B_z values yielding $n = 11$ or 12. The phases were calculated by the method described in an earlier paper.¹³ The appropriate n -crit value of 11.5 is seen to be compatible with the calculations at higher and lower B_z . Similar check calculations were carried out in other ranges of B_z . It is noted that the convergence of this procedure is inferior to that of the iterative method since: (1) for each B_z a series of phases is required, and (2) the series must be extended to $K < 2 \times 10^{-6}$ if n is to be determined with certainty.

¹² See P. Swan, *Proc. Roy. Soc. (London)* **A228**, 10 (1955).

¹³ R. B. Bernstein, *J. Chem. Phys.* **33**, 795 (1960).

TABLE VI. Expansion coefficients for $V^*(\xi) = a_0\xi^2 (1 + a_1\xi^1 + \dots + a_6\xi^6) - 1$, $\xi = z - 1$.

	a_0	a_1	a_2	a_3	a_4	a_5	a_6
L-J (12.000,6)	36.0000	-7.00000	30.9167	-107.333	318.111	-840.000	2028.00
Exp (12.000,6)	30.0000	-5.86667	20.4000	-52.370	107.440	-184.183	269.67
Exp (13.772,6)	36.0000	-6.57944	25.9415	-76.132	180.479	-360.836	624.94
Exp (15.000,6)	40.0000	-7.04167	29.9062	-94.969	244.422	-532.011	1005.77
Morse (6)	36.0000	-6.00000	21.0000	-54.000	111.600	-194.400	293.91

Eigenenergies

Figure 1(b) presents a simplified flow diagram for the computation of $-K$. Here, B_z is fixed and an initial value of $-K$ is improved by iteration. The remarks of the earlier section concerning tests of initial boundary condition and size of the integration step, H , also apply

to the eigenenergy calculations, for which the precision was $\pm 5 \times 10^{-6}$.

Results of these computations are collected in Tables III and IV. In Table III the bound-state energy levels are compared for the several potentials at a common B_z , 2500, a value corresponding to a light "chemically bound" or heavy "van der Waals" diatom.

TABLE VII. Dunham expansion coefficients for: $K(v) = -1 + \sum_{i=0}^4 C_i(B_z)\phi^i$.

		$B_z=100$	$B_z=900$	$B_z=2500$	$B_z=10\ 000$
C_0	L-J (12,6)	0.008750	0.000972	0.000350	0.000088
	Exp (12,6)	0.001211	0.000135	0.000048	0.000012
	Exp (13.772,6)	0.002586	0.000287	0.000103	0.000026
	Exp (15,6)	0.003681	0.000409	0.000147	0.000037
	Morse (6)	0.000000	0.000000	0.000000	0.000000
C_1	L-J (12,6)	11.9671	11.9963	11.9987	11.9997
	Exp (12,6)	10.9640	10.9555	10.9548	10.9545
	Exp (13.772,6)	12.0123	12.0014	12.0005	12.0001
	Exp (15,6)	12.6639	12.6508	12.6497	12.6493
	Morse (6)	12.0000	12.0000	12.0000	12.0000
C_2	L-J (12,6)	-45.5276	-45.5030	-45.5011	-45.5002
	Exp (12,6)	-33.9135	-33.9311	-33.9325	-33.9331
	Exp (13.772,6)	-42.2437	-42.2536	-42.2544	-42.2547
	Exp (15,6)	-48.1205	-48.1135	-48.1130	-48.1127
	Morse (6)	-36.0000	-36.0000	-36.0000	-36.0000
C_3	L-J (12,6)	48.8711			
	Exp (12,6)	8.6971			
	Exp (13.772,6)	18.1388			
	Exp (15,6)	26.9450			
	Morse (6)	0.0000			
C_4	L-J (12,6)	29.1645			
	Exp (12,6)	29.0775			
	Exp (13.772,6)	55.1785			
	Exp (15,6)	79.6992			
	Morse (6)	0.0000			

For potential expansions with terms no higher than a_6 , the coefficients C_3 and C_4 are not functions of B_z .

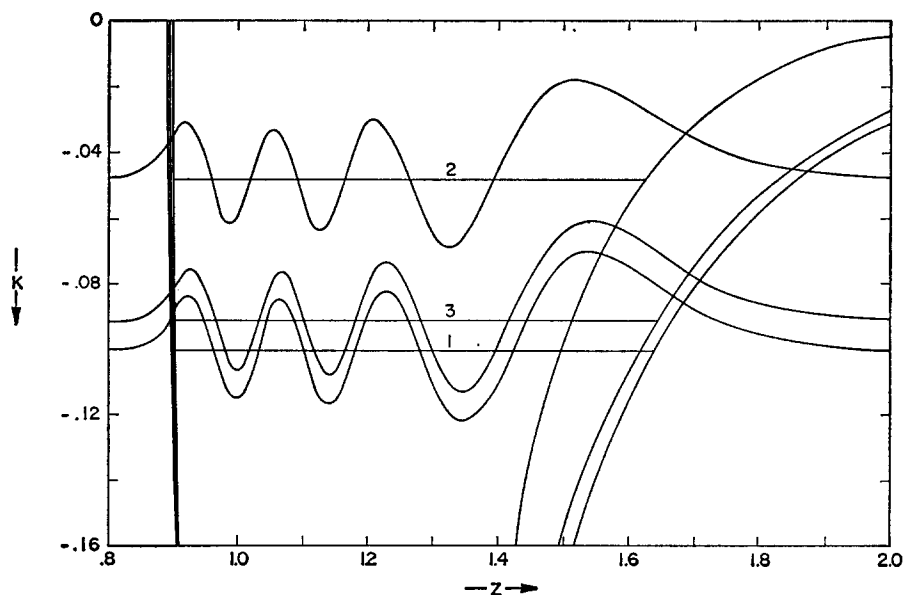


FIG. 3. Wavefunctions for $v=6$: Plotted is $Y(z)=z \cdot R(z)$. (1) L-J (12, 6), (2) Morse (6), (3) exp (13.772, 6).

In Table IV the effect of B_z upon the number of states and their energies is shown for the L-J(12, 6) potential in columns headed "Eigen," together with levels obtained by first-order WKBJ and the Dunham form of the second-order WKBJ approximation, as will be discussed in the succeeding paragraphs.

Test of the First-Order WKBJ Approximation

The first-order WKBJ approximation may be written

$$\phi = B_z^{-1}(v + \frac{1}{2}) = \frac{1}{\pi} \int_{z_a}^{z_b} [K - V_\theta^*(z)]^{1/2} dz, \quad (4)$$

where z_a and z_b are the classical turning points, $V_\theta^*(z) = V^*(z) + \theta z^{-2}$, and $\theta = (l + \frac{1}{2})^2 / B_z$. The necessary modification in (4) whereby $(l + \frac{1}{2})^2$ is substituted for $l(l+1)$, including the case $l=0$, is discussed by Langer,¹⁴ whose name it is sometimes given.¹⁵

The integral is readily computed for various values of K and θ , thus permitting a facile interpolation to find K for a given B_z with arbitrary l and v . Arrays of the integral, ϕ , are presented in Table V. The integrations were performed by Simpson's rule quadrature with 100 cuts for $K < -0.1$ and 150 cuts otherwise. To use the tables for a given B_z , v and l , one forms ϕ and θ ; then by linear interpolation between both rows and columns one obtains K . In Table IV energies by this procedure are compared with the more accurate values by the iterative method.

¹⁴ R. E. Langer, Phys. Rev. **51**, 669 (1937).

¹⁵ Should we then label the method WKBJL? The modification was recognized by Kramers as early as 1926, however. See the remarks of Beckel.¹⁶

¹⁶ C. L. Beckel and J. Nakhleh, Phys. Rev. (to be published).

Dunham Form of Second-Order WKBJ Approximation

A particularly simple treatment is available¹⁷ for potentials with a single minimum which can be expanded in the anharmonic series:

$$V^*(\xi) = -1 + a_0 \xi^2 (1 + a_1 \xi + a_2 \xi^2 \cdots a_n \xi^n), \quad (5)$$

where $\xi = z - 1$. For five of the present potentials, $a_0 \cdots a_6$ are given in Table VI.

Dunham has applied the second-order WKBJ treatment to (5), expressing the eigenenergies as,

$$F(v, l) = (K+1)\epsilon/hc = \sum_{i,j} Y_{ij}(v + \frac{1}{2})^i [l(l+1)]^j, \quad (6)$$

and has evaluated fifteen lower Y_{ij} 's in terms of B_e and $a_0 \cdots a_6$. To compare with results from the iterative and first-order WKBJ methods, and to remove the greater part of the dependence of the Y 's upon B_e , we transpose (6) to yield, for $l=0$,

$$K = -1 + \sum_{i=0}^4 C_i(B_z) \phi^i, \quad (7)$$

with, again, $\phi = B_z^{-1}(v + \frac{1}{2})$.

Table VII lists values of $C_i(B_z)$ for the L-J(12, 6), Morse (6), and three exptl(α , 6) potentials, each for four values of B_z . For comparison with the iterative and first-order WKBJ methods, the energies from (7) are listed in Table IV.

DISCUSSION

Considerations of precision and cost are relevant to choice of method for approximate solution of the wave equation. The precision of the present iterative method

¹⁷ J. L. Dunham, Phys. Rev. **41**, 721 (1932).

is a nearly linear function of the number of trials, about three trials or four machine seconds (IBM 7090) per significant figure in K (or B_z); in the present work K was calculated with an accuracy of $\pm 5 \times 10^{-6}$, and $B_{z\text{-crit}}(v)$ to ± 0.1 . The WKB methods give eigenenergies of lower accuracy, but are considerably faster. [See, however, subsequent cautionary remarks regarding the failure of the WKB method for evaluating $B_{z\text{-crit}}(v)$.] Therefore the iterative method appears more suitable when four or more significant figures in K are required. Because the iterative method can be used to generate eigenvalues of very high numerical accuracy, however, the user should be aware of possible limitation by the Born–Oppenheimer approximation. The generality of the method and the ease of adapting to new potentials should be noted.

An important product of the computation is the generation of wavefunctions. For illustration, Fig. 3 shows the functions, $Y(z) = zR(z)$, scaled to be equal at the outermost maximum, for the sixth vibrational state of the matched potentials: L-J(12, 6), $\exp(13.772, 6)$, and Morse(6). Indeed, where reasonably accurate eigenenergies are known, as for example with the Morse potential, a single pass through the iterative routine will ordinarily produce the wavefunction more simply than by the conventional expansion. The inverse process, reducing numerical wavefunctions from the iterative technique into expansions in terms of, for example, Hermite polynomials, should be computationally straightforward.

Several remarks are in order concerning the WKB methods. Two criteria for the accuracy of the first-order integral, Eq. (4), are that the potential change slowly within a wavelength, and that the interval of integration be greater than a wavelength. For the potentials to which the method was applied, the first condition is met over the greater part of the well, though not at the interior turning point, but the second condition is violated both for the lowest and the highest of the bound states. Thus the first-order WKB treatment can be expected to be, and is most accurate for the middle states (see Table IV). The failure for the upper states makes estimation of $B_{z\text{-crit}}$ by first-order WKB to be of little value. Estimates high by as much as 30% were obtained, compared with the results of Table I.

For the lower states (those for which $K < -0.1$),

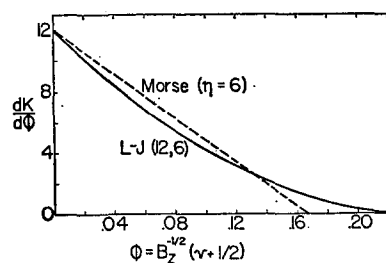


FIG. 4. Reduced Birge–Sponer diagrams. Note:

$$\int_0^{\phi_{\max}} (dK/d\phi) d\phi = 1.$$

the Dunham treatment is seen to give excellent agreement with the iterative calculation. Near the top of the well, however, serious discrepancies occur in both the magnitude of the energies and the sense of their differences. In fact, the series of K 's goes through a spurious maximum, probably arising from the failure of the Eq. (5) to converge for potentials having z^{-6} dependence. Indeed, the series fails to converge for $z \geq 2$, a delinquency which obscures the test of improvement due to the second-order WKB integral.¹⁸ Attempts have been made⁶ to extend the Dunham method by computing the higher Y_{ij} 's of Eq. (6), but a number of difficulties remain.¹⁶

Finally, we wish to remark about the degree to which the L-J($n, 6$) and $\exp(\alpha, 6)$ potentials are "realistic." Figure 4 shows a reduced Birge–Sponer diagram for the L-J(12, 6) and Morse(6) potentials. The former potential shows everywhere a positive curvature, a feature shared by similar plots for the exponential potentials. Most experimental Birge–Sponer diagrams have regions of negative curvature, however. Although positive curvature is expected at high v , such curvature everywhere does not accord with experiment. It should therefore be emphasized that in the present paper a powerful method has been applied to still approximate potentials.

ACKNOWLEDGMENT

The authors wish to thank Mr. Arnold Flank for his assistance with the computations.

¹⁸ The nonconvergence for r^{-6} potentials is shared by a recent second-order perturbation calculation: A. M. Shorb, R. Schroeder, and E. R. Lippincott, *J. Chem. Phys.* **37**, 1043 (1962).